

Revue des Composites et des Matériaux Avancés-Journal of Composite and Advanced Materials

Vol. 35, No. 5, October, 2025, pp. 1003-1008

Journal homepage: http://iieta.org/journals/rcma

Optical and Structural Characterization of NiO Nanoparticles Prepared by Plasma Jet Method



Mohammed Kh. Ibrahim¹, Bilal K. Al-Rawi^{2*}

- ¹ Ministry of Education, Anbar Education Directorate, Al Rumadi 31001, Iraq
- ² Department of Physics, College of Education for Pure Science, University of Anbar, Al Rumadi 31001, Iraq

Corresponding Author Email: sc.bilal alrawi@uoanbar.edu.iq

Copyright: ©2025 The authors. This article is published by IIETA and is licensed under the CC BY 4.0 license (http://creativecommons.org/licenses/by/4.0/).

https://doi.org/10.18280/rcma.350520

Received: 11 June 2025 Revised: 18 June 2025 Accepted: 30 July 2025

Available online: 31 October 2025

Keywords:

plasma jet, NiO nanoparticles, structural properties, optical properties

ABSTRACT

Significant research attention has been directed toward nanomaterials because of their broad utility in diverse fields. The techniques used for their synthesis play a pivotal role in defining their resultant physical and chemical characteristics. In this study, nanoscale nickel oxide (NiO) particles were synthesized using a plasma jet technique. The plasma jet method represents an innovative, fast, and solvent-less pathway for nanoparticle fabrication. This stands in stark contrast to traditional approaches like sol-gel and hydrothermal processes, which are often characterized by extended reaction durations and the requirement for chemical precursors. This synthesis technique proves to be both highly efficient and readily scalable, facilitating the generation of superior-quality NiO nanoparticles characterized by regulated dimensions and negligible impurities. The high purity of the resultant nanoparticles was verified via X-ray diffraction (XRD) and energydispersive X-ray spectroscopy (EDX). The XRD pattern displayed well-defined peaks at 2θ angles of 37.19°, 43.28°, 62.69°, and 75.39°, which are indexed to the (111), (200), (220), and (311) planes, respectively, affirming the cubic face-centered crystalline phase of NiO. Application of the Scherrer equation to this data yielded an average crystallite size of roughly 15.67 nm. Complementary morphological studies were conducted using atomic force microscopy (AFM) and field emission scanning electron microscopy (FESEM). AFM measurements determined an average grain size of 83.10 nm. The FESEM micrographs further revealed that the nanoparticles possessed a spherical morphology, were effectively dispersed, and had a mean particle diameter of 65.30 nm. Optical characterization revealed that the NiO nanoparticles exhibited a direct optical band gap of 3.90 eV, indicating their potential for applications in optoelectronic devices.

1. INTRODUCTION

The unique physicochemical properties of Atmospheric Pressure Plasma Jets (APPJs) have generated considerable global research interest. The efficacy of these jets in different applications is governed by a fundamental interplay between plasma physics, plasma chemistry, and fluid dynamics [1]. Research has demonstrated that plasma jets are capable of producing a high concentration of reactive species while maintaining relatively low gas temperatures. As a result, they have been explored for numerous uses, including polymer etching, food sterilization, and the treatment of water and biological tissues [2]. In recent times, plasma-based methods have risen in prominence as environmentally friendly techniques for synthesizing nanomaterials, advantages over traditional solid, liquid, and gas-phase synthesis methods [3]. Nanoparticles exhibit distinct electronic, optical, chemical, and biological characteristics that set them apart from their bulk material forms. Properties such as electrical conductivity and resistivity, mechanical strength and hardness, diffusion behavior, chemical reactivity,

biological effectiveness differ notably between nanoparticles and larger-scale materials [4]. The diverse functionalities of nano-structured metal oxide substances, including their optical, magnetic, electrical, and catalytic properties, have attracted considerable interest. These remarkable attributes contribute to a wide range of potential applications across various fields [5]. Nickel oxide (NiO) is recognized for its remarkable chemical stability. Owing to its exceptional chemical stability, cost-effectiveness, and superior ion storage capacity, nickel oxide (NiO) has become a subject of intensive study [6]. NiO nanoparticles exhibit ptype conductivity, attributed to their wide band gap ranging between 3.6 and 4.0 eV [7, 8]. These nanoparticles find use across multiple fields, including photocatalysis, battery technology, electrochromic devices, chemical sensors [9-11] and gas sensing applications [12]. Various synthesis methods have been employed to produce NiO nanoparticles. Conventional methods, such as sol-gel and hydrothermal approaches, often require lengthy processing times, complex chemical reactions, and post-synthesis treatments that can introduce impurities or alter material quality. In contrast, the plasma jet method offers a novel and efficient synthesis route that does not rely on chemical precursors or surfactants. This technique enables the rapid formation of nanoparticles through high-energy plasma discharge in a controlled environment, resulting in high-purity products with minimal surface contamination [13-15]. This study employs the plasma jet technique to synthesize nickel oxide nanoparticles, followed by the examination of their optical and structural characteristics.

2. EXPERIMENTAL WORK

The experimental setup, illustrated in Figure 1, features a non-thermal plasma jet operating at atmospheric pressure. The diagram includes an inset highlighting the jet's tip, from which argon gas is discharged into a beaker. Within this beaker, a nickel strip (7 cm × 1 cm) submerged in 5 ml of deionized water serves as the precursor material. With the plasma nozzle fixed 2 cm above the water's surface, the argon flow interacts with the aqueous medium, initiating surface reactions on the nickel strip that ultimately yield metal nanoparticles. Nanoparticles were generated during a 6-minute period, with pure argon gas (purity 99.99%) flowing at 2 liters per minute

and an applied voltage of 16 kV. The plasma needle was held vertically above the beaker where the metal strip was submerged in deionized water. The operating parameters for the plasma jet were optimized through initial tests to ensure a stable plasma discharge and reproducible nanoparticle synthesis. These settings were found to provide a reliable arc generation with minimal fluctuation, ensuring effective energy transfer to the nickel precursor and facilitating nanoparticle synthesis. The duration of plasma exposure plays a significant role in determining the final particle size. Extended plasma duration typically leads to increased particle growth due to prolonged nucleation and coalescence. The formation mechanism of NiO nanoparticles in the plasma jet process involves three main steps: nucleation of Ni atoms due to highenergy plasma, growth through particle collision and coalescence, and subsequent oxidation upon exposure to ambient oxygen. After synthesizing NiO nanoparticles, thin films were prepared to examine their characteristics. Glass substrates sized 3 × 2 cm² were used and underwent thorough cleaning in an ultrasonic bath for 10 minutes with distilled water and alcohol to remove contaminants. The nanoparticle dispersion was then deposited onto the substrates through the drop-casting technique.

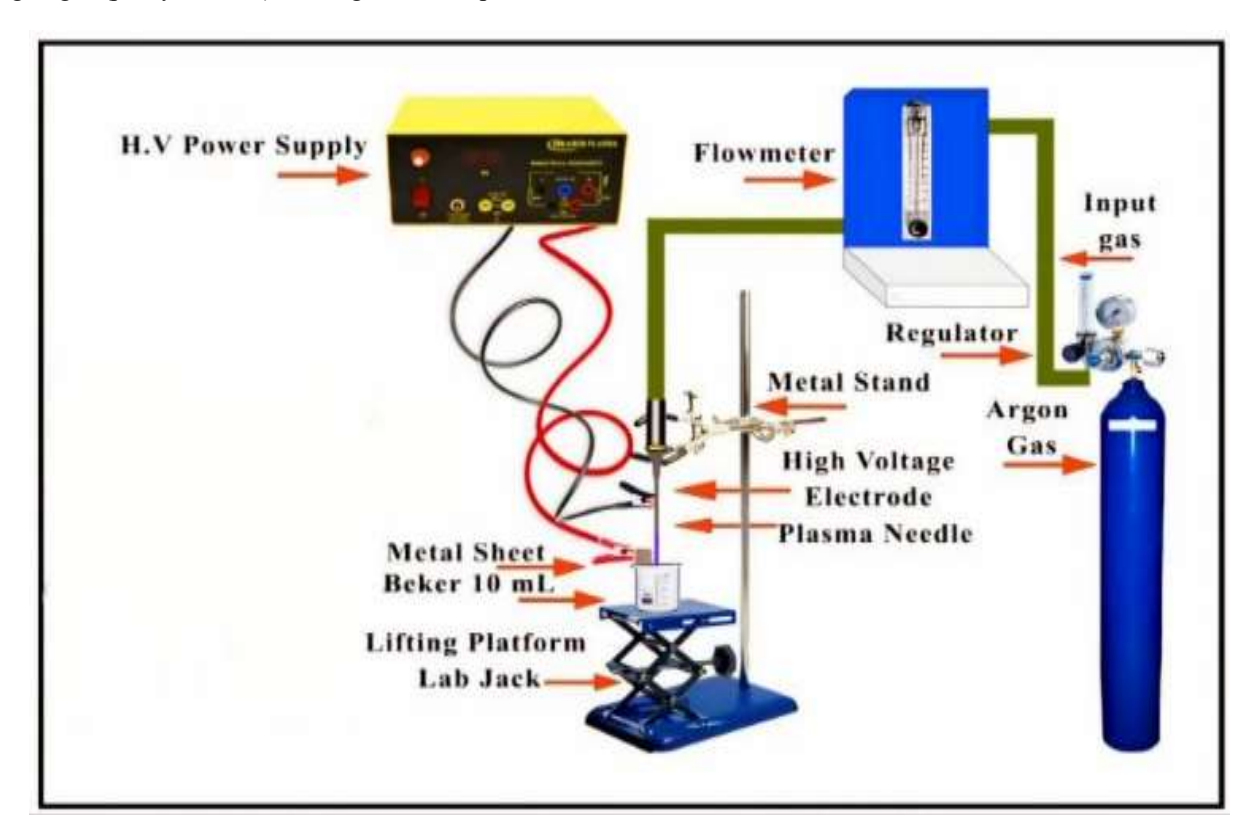


Figure 1. A cross-sectional diagram of the experimental arrangement for the atmospheric plasma jet

3. RESULT AND DISSECTION

The crystalline structure of the synthesized material was examined using X-ray diffraction (XRD). This technique operates on the principle that X-rays diffract from crystalline lattices, producing a pattern that reveals the atomic arrangement. The crystal structure of the deposited NiO nanoparticles was determined by XRD, with the resulting pattern displayed in Figure 2. Distinct diffraction peaks were identified at 2θ values of 37.19° , 43.28° , 62.69° , and 75.39° .

These peaks respectively correspond to the (111), (200), (220), and (311) planes, matching the known pattern for a face-centered cubic NiO lattice as per JCPDS No. 00-047-1049 [16]. The lack of extraneous diffraction peaks indicates that the produced NiO possesses a high degree of phase purity. These findings align well with results from atomic force microscopy (AFM), field emission scanning electron microscopy (FESEM), and EDX analyses [17, 18]. further confirming the quality and structure of the prepared NiO films. Details of the XRD peak positions and intensities are provided

in Table 1.

Figure 3 illustrates the development of the surface topography for the NiO nanoparticles sample. The accompanying histogram provides information about the average particle size of the NiO nanoparticles, while the three-dimensional image reveals details about the surface morphology and roughness. The NiO thin film, produced via the plasma jet technique, exhibits a uniform surface with grains oriented perpendicularly in an elongated form. Due to the high sensitivity of the AFM technique to variations in local surface height, surface roughness parameters such as root-mean-square (RMS) roughness and grain size were determined from the AFM height data. Analysis yielded an RMS value of 15.14 nm, a Sa roughness of 10.17 nm, and an average grain size measuring 83.10 nm, based on a scanned area of 4.25 μm by 4.25 μm .

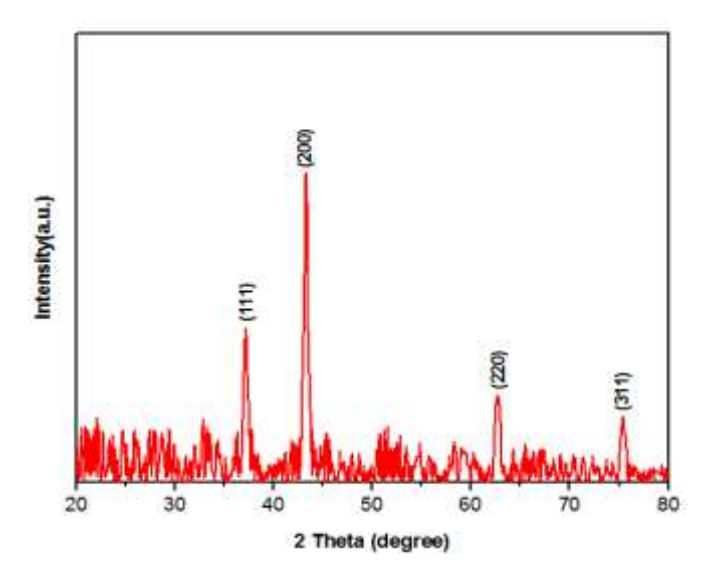


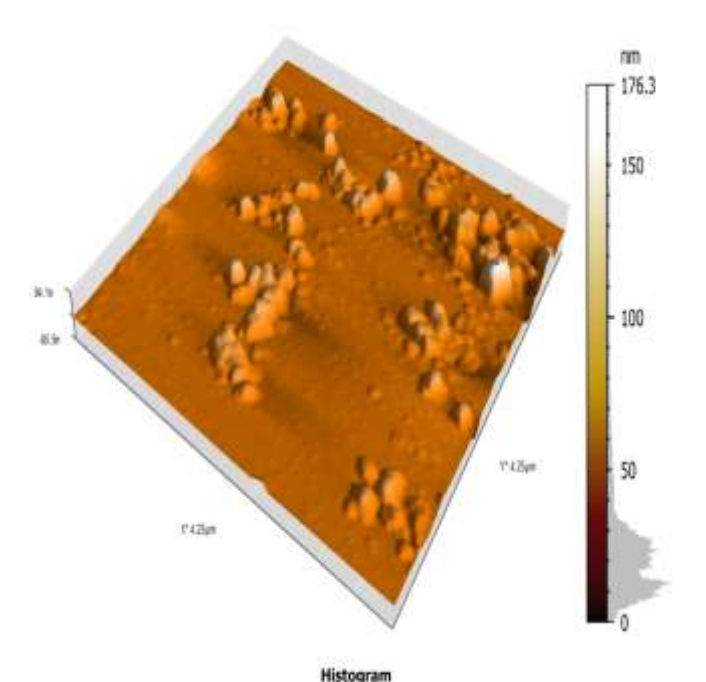
Figure 2. The X-ray diffraction patterns for the plasma-jet-synthesized NiO nanoparticles

Table 1. Overview of X-ray analysis results

Gas Flow Rate (L/min	20 Angl e (°)	FWH M (°)	Experiment al d-spacing (Å)	Crystallit e Size (nm)	Miller Indice s (hkl)
	37.19	0.5582	2.4157	15	(111)
2	43.28	0.4507	2.0888	19	(200)
	62.69	0.6632	1.4808	14	(220)
	75.39	0.6833	1.2598	14.7	(311)

Figure 4 illustrates the detailed microscopic surface structure of NiO nanoparticles. The surface morphology was examined using FESEM on NiO nanoparticles synthesized via a plasma jet method. The image reveals the level of magnification applied during the FESEM analysis. Upon close inspection, the nanostructure appears to consist of roughly spherical particles, suggesting a uniform size distribution and good dispersion throughout the sample preparation. The average diameter of these nanoparticles was measured to be approximately 65.30 nm. Due to the agglomeration of multiple crystallites. The crystallite size of NiO nanoparticles calculated from XRD using the Scherrer equation was 15.67 nm. This difference is common in plasma jet-synthesized nanoparticles and is caused by the distinction between crystallite size XRD and agglomerate size FESEM.

The elemental composition of the synthesized nickel oxide nanoparticles was analyzed using energy-dispersive X-ray spectroscopy (EDX) [19]. Figure 5 illustrates the EDX spectrum of the NiO nanoparticles at the microscopic scale, accompanied by a table presenting the quantitative results. The analysis reveals peaks corresponding only to nickel and oxygen, with mass percentages of 86.86% and 13.14%. respectively. The EDX spectrum showed no signs of elemental contaminants above its detection threshold, thereby corroborating the synthesis of highly pure and crystalline NiO nanoparticles—a finding that aligns with the XRD results. It is important to acknowledge, however, the inherent constraints of the EDX technique. Its detection capability is generally limited to concentrations above approximately 0.1 wt.%, and it is less effective at identifying light elements or trace impurities. Consequently, the potential existence of minor surface adsorbates or undetectable contaminants, while unlikely to be significant, cannot be completely excluded.



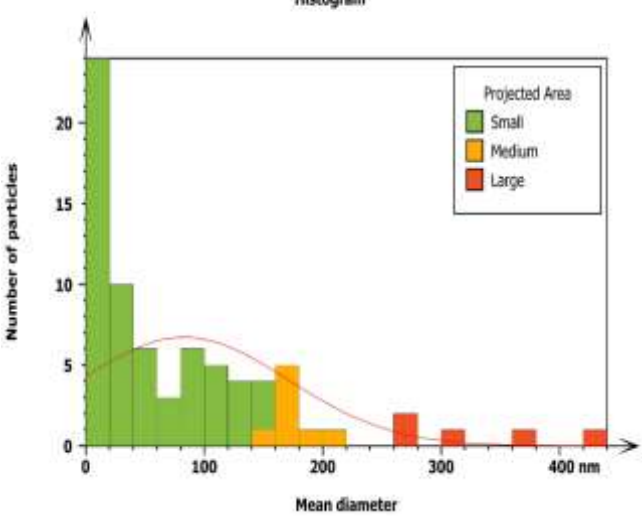


Figure 3. Three-dimensional image of NiO nanoparticles obtained by AFM, along with their size distribution histogram, prepared using a plasma jet

The optical absorption properties of the synthesized NiO nanoparticles were investigated using UV-vis spectroscopy,

as shown in Figure 6. The spectrum is characterized by a strong absorption feature in the ultraviolet range, with a well-defined edge near 400 nm. This prominent absorption edge indicates effective UV light absorption by the nanoparticles and points to a high degree of crystallinity and a narrow size distribution [20-22]. These optical characteristics are in strong agreement with the structural and morphological data provided by the XRD and FESEM results. The optical band gap energy was subsequently determined from this data by applying Eq. (1), illustrated in Figure 7.

$$(\alpha h v) = A (h v - Eg)^n$$
 (1)

In this context, α denotes the absorption coefficient of the

material, h is Planck's constant, v represents the frequency, Eg stands for the band gap energy, A is a proportionality constant, and n indicates the nature of the electronic transitions (whether direct or indirect) in the sample [23]. The optical energy band gap of NiO is measured to be 3.90 eV. This widening can be attributed primarily to quantum confinement effects arising from the nanoscale crystallite size, as confirmed by XRD. When the particle size approaches the exciton Bohr radius, the electronic band structure is altered, leading to an increase in band gap energy. Additionally, the uniform morphology and low surface defect density. This value for NiO nanoparticles is consistent with the findings reported in references [24, 25], and is in good agreement with the results obtained from XRD and FESEM analyses.

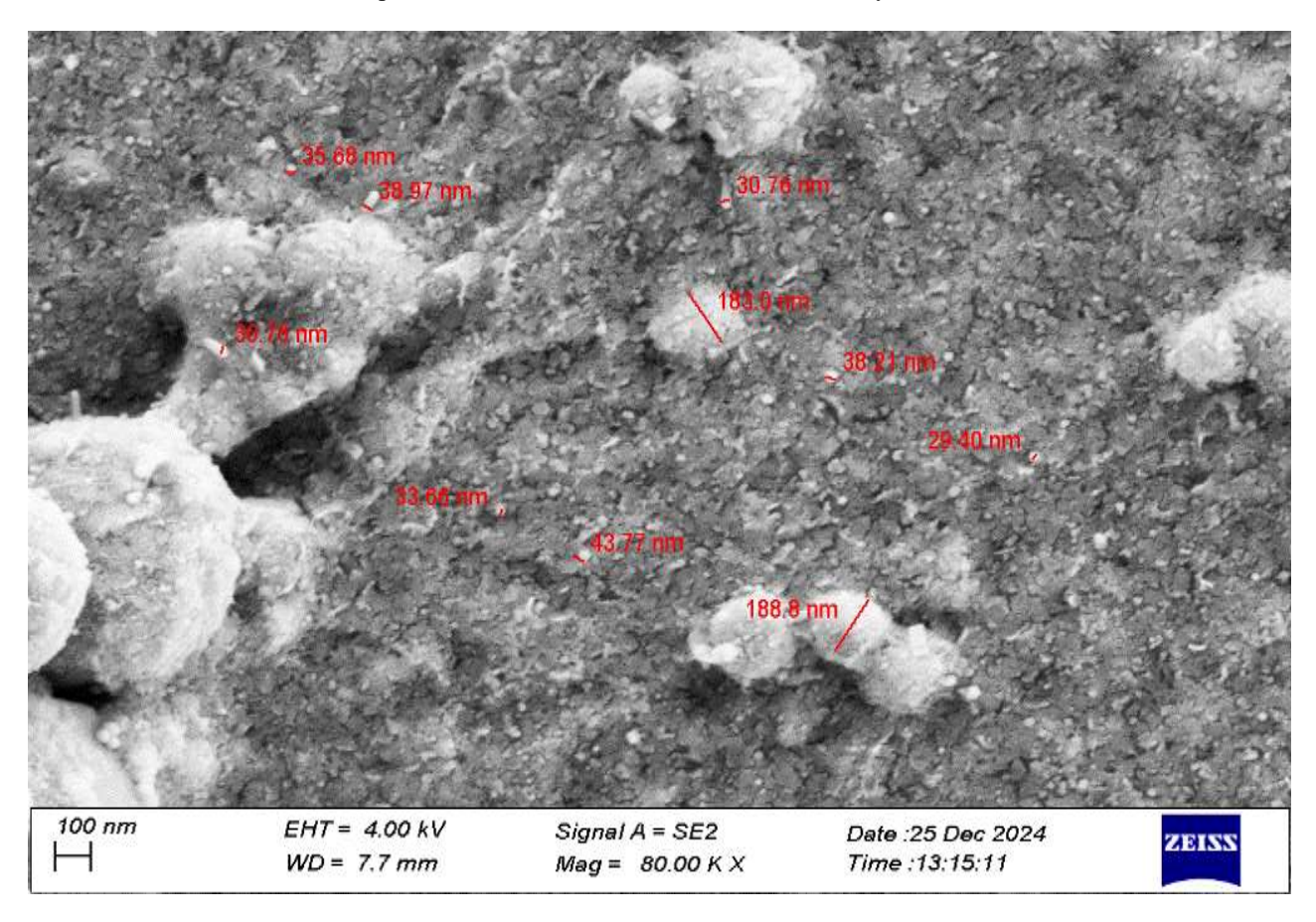


Figure 4. FE-SEM morphology of NiO nanoparticles from plasma jet synthesis

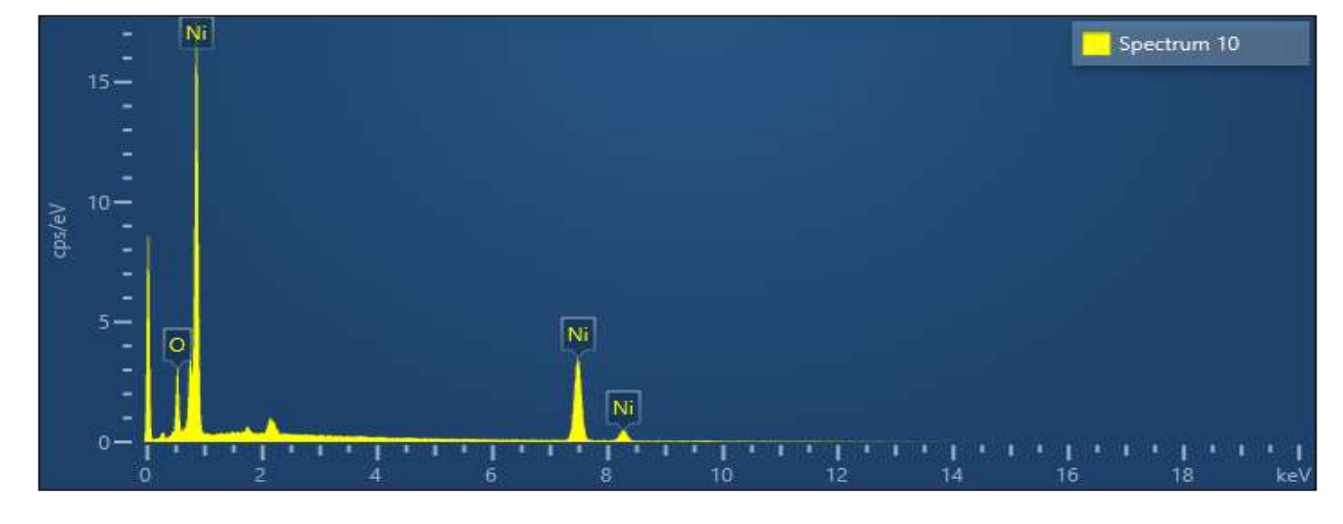


Figure 5. EDX spectrum confirming the elemental purity of nickel oxide nanoparticles produced by the plasma jet technique

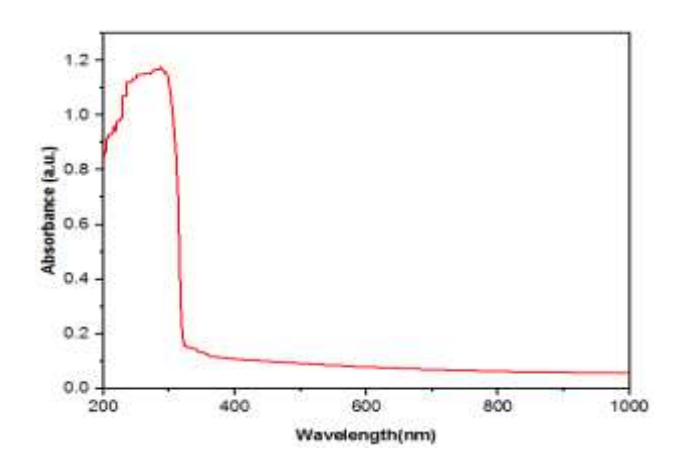


Figure 6. UV-Vis absorption profile of plasma jetsynthesized NiO nanoparticles

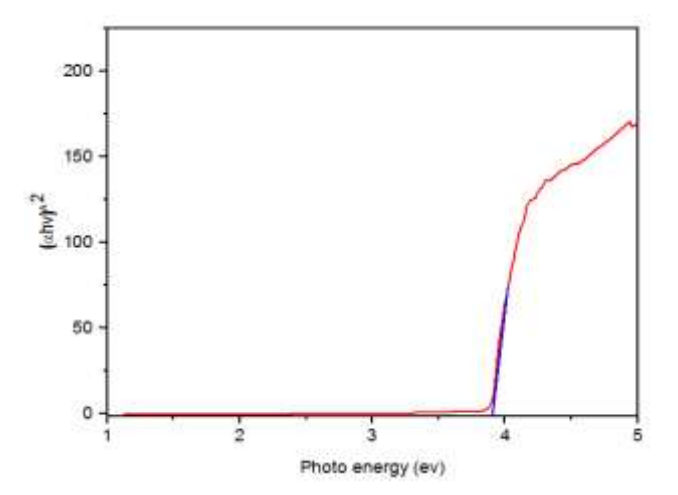


Figure 7. Tauc plot analysis for calculating the optical band gap of nickel oxide nanoparticles fabricated via a plasma jet

4. CONCLUSION

In summary, the plasma jet approach establishes itself as a sustainable, economical, and adaptable route for producing high-purity NiO nanoparticles. Structural characterization by XRD verified the successful formation of a face-centered cubic crystal phase. Morphological examination using AFM indicated a smooth and uniform film surface, featuring threedimensionally perpendicular grain alignment that denotes a well-ordered architecture. FESEM observations confirmed a primarily spherical nanoparticle geometry with a propensity for cluster formation, while EDX spectrometry provided additional evidence of the material's high purity. From an optical standpoint, the measured band gap of 3.90 eV underscores the potential of these nanoparticles in optoelectronics and energy conversion technologies. Their significant transparency further positions them as promising candidates for ultraviolet photodetectors and specialized optical coatings. Moreover, the combined attributes of excellent crystallinity and purity render them highly appropriate for roles as p-type semiconductors in transparent electronic components and as hole transport layers in photovoltaic cells. Collectively, these results suggest that NiO nanoparticles produced via the plasma jet technique could offer enhanced performance and broader application potential compared to those synthesized by conventional methods.

Although the primary goal of this work was to investigate the structural and optical properties of NiO nanoparticles synthesized by the plasma jet method, the long-term stability and batch-to-batch reproducibility were not systematically studied. Therefore, future work should focus on evaluating the aging behavior and reproducibility under varying environmental conditions to confirm the practical reliability of the synthesized nanoparticles.

REFERENCES

- [1] Shalaan, M.M., Khalaf, M.K., Al-Rawi, B.K. (2024). Study of gold doping in optical and electrical properties of tungsten trioxide thin films deposited by spray method. Journal of Optics, 53(5): 4571-4578. https://doi.org/10.1007/s12596-024-01701-8
- [2] Al-Rawi, B.K., Hameed, S.M., Alsaadi, M.A.M. (2021). Simulation of electronic structure and some properties of CdTe crystals using DFT. Materials Science Forum, 1021: 1-10. https://doi.org/10.4028/www.scientific.net/MSF.1021.1
- [3] Kaushik, N.K., Kaushik, N., Linh, N.N., Ghimire, B., Pengkit, A., Sornsakdanuphap, J., Lee, S.J., Choi, E.H. (2019). Plasma and nanomaterials: Fabrication and biomedical applications. Nanomaterials, 9(1): 98. https://doi.org/10.3390/nano9010098
- [4] Khashan, K.S., Sulaiman, G.M., Hamad, A.H., Abdulameer, F.A., Hadi, A. (2017). Generation of NiO nanoparticles via pulsed laser ablation in deionised water and their antibacterial activity. Applied Physics A, 123(3): 190. https://doi.org/10.1007/s00339-017-0826-4
- [5] Mohammed, S.A.J., Al-Haddad, R.M., Al-Rawi, B.K. (2024). Structural and optical properties of magnetite nanoparticles prepared by green method for biophysics applications. Nanoscience and Technology: An International Journal, 15(2): 95-105. https://doi.org/10.1615/NanoSciTechnolIntJ.202304838
- [6] Kafel, A., Al-Rashid, S.T. (2023). Examining the impact of quantum confinement energy on the optical characteristics of zinc sulfide and gallium nitrate in the ultraviolet spectral range. Chalcogenide Letters, 20(6): 423-429. https://doi.org/10.15251/CL.2023.206.423
- [7] Fahad, O.A., Al-Rawi, B.K., Ramizy, A., Salih, E.Y. (2025). High-performance ZnO/CdTe/Ge/Si heterojunction photodetector for short/mid-wavelength detection. Sensors and Actuators A: Physical, 383: 116198. https://doi.org/10.1016/j.sna.2025.116198
- [8] Yousaf, S., Zulfiqar, S., Shahi, M.N., Warsi, M.F., Al-Khalli, N.F., Aboud, M.F.A., Shakir, I. (2020). Tuning the structural, optical and electrical properties of NiO nanoparticles prepared by wet chemical route. Ceramics International, 46(3): 3750-3758. https://doi.org/10.1016/j.ceramint.2019.10.097
- [9] Al-Rashid, S.N.T. (2024). Study of the variations of quantum confinement energy with the exciton Bohr radius of zinc selenide. Nanoscience and Technology: An International Journal, 15(3): 21-27. https://doi.org/10.1615/NanoSciTechnolIntJ.202304864
- [10] Mahmoud, S.A., Shereen, A., Mou'ad, A.T. (2011). Structural and optical dispersion characterisation of sprayed nickel oxide thin films. Journal of Modern

- Physics, 2(10): 8057. https://doi.org/10.4236/jmp.2011.210147
- [11] Rani, B.J., Ravi, G., Yuvakkumar, R., Ravichandran, S., Ameen, F., Al-Sabri, A. (2019). Efficient, highly stable Zn-doped NiO nanocluster electrocatalysts for electrochemical water splitting applications. Journal of Sol-Gel Science and Technology, 89(2): 500-510. https://doi.org/10.1007/s10971-018-4886-5
- [12] Nakate, U.T., Lee, G.H., Ahmad, R., Patil, P., Bhopate, D.P., Hahn, Y.B., Yu, Y.T., Suh, E.K. (2018). Hydrothermal synthesis of p-type nanocrystalline NiO nanoplates for high response and low concentration hydrogen gas sensor application. Ceramics International, 44(13): 15721-15729. https://doi.org/10.1016/j.ceramint.2018.05.246
- [13] Mohammed, R.S., Aadim, K.A., Ahmed, K.A. (2022). Synthesis of CuO/ZnO and MgO/ZnO core/shell nanoparticles with plasma jets and study of their structural and optical properties. Karbala International Journal of Modern Science, 8(2): 88-97. https://doi.org/10.33640/2405-609X.3225
- [14] Ibrahim, M.K., Al-Rawi, B.K. (2025). Influence of gas flow rate on the structural and optical properties of TiO₂ prepared by plasma jet technique. Revue des Composites et des Matériaux Avancés, 35(4): 629-634. https://doi.org/10.18280/rcma.350404
- [15] Al-Ariki, S., Yahya, N.A., Al-A'nsi, S.A.A., Jumali, M.H., Jannah, A.N., Abd-Shukor, R. (2021). Synthesis and comparative study on the structural and optical properties of ZnO doped with Ni and Ag nanopowders fabricated by sol gel technique. Scientific Reports, 11(1): 11948. https://doi.org/10.1038/s41598-021-91439-1
- [16] Shalaan, M.M., Khalaf, M.K., Al-Rawi, B.K. (2024). Impact of gold nanoparticles doping on the characterization of vacuum ultraviolet MSM detector utilizing tungsten trioxide thin film. Journal of Optics, pp. 1-12. https://doi.org/10.1007/s12596-024-02047-x
- [17] Mustafa, A., Al-Rashid, S.T. (2024). Cohesive energy model for the optical properties in nanostructured materials of zinc sulfide and cadmium selenide. Chalcogenide Letters, 21(5): 407-411. http://doi.org/10.15251/CL.2024.215.407
- [18] Mohammed, S.A.J., Al-Haddad, R.M., Al-Rawi, B.K.

- (2024). NIR laser effect on cancer cell lines activity by using $Fe_3O_4@Cu@SiO_2$ core—shell nanoparticles. Journal of Optics, 54: 414-421. https://doi.org/10.1007/s12596-024-01676-6
- [19] Shamim, A., Ahmad, Z., Mahmood, S., Ali, U., Mahmood, T., Nizami, Z. (2019). Synthesis of nickel nanoparticles by sol-gel method and their characterization. Open Journal of Chemistry (OJC), 2: 16-20. http://doi.org/10.30538/psrp-ojc2019.0009
- [20] Racik, K.M., Madhavan, J., Raj, M.V.A. (2018). Synthesis, characterization and optical properties of spherical NiO nanoparticles. In National Laser Symposium (NLS-27), RRCAT, pp. 1-6.
- [21] Uddin, M.T., Nicolas, Y., Olivier, C., Jaegermann, W., Rockstroh, N., Junge, H., Toupance, T. (2017). Band alignment investigations of heterostructure NiO/TiO₂ nanomaterials used as efficient heterojunction earth-abundant metal oxide photocatalysts for hydrogen production. Physical Chemistry Chemical Physics, 19(29): 19279-19288. https://doi.org/10.1039/C7CP01300K
- [22] Noor, S., Sajjad, S., Leghari, S.A.K., Long, M. (2020). Energy harvesting for electrochemical OER and solar photocatalysis via dual functional GO/TiO₂-NiO nanocomposite. Journal of Cleaner Production, 277: 123280. https://doi.org/10.1016/j.jclepro.2020.122926
- [23] Hussain, A.M., Al-Rawi, B.K. (2024). Study the optical and Antibacterial properties of the Ag nano-particles by exploding of wire technique. Journal of University of Anbar for Pure Science, 18(1): 197-202. https://doi.org/10.37652/juaps.2023.143290.1133
- [24] Khathim, S.A.E., Al-Rawi, B.K., Khalaf, M.K. (2023). Antibacterial activity of NiTi alloy with sputtered tantalum. Journal of University of Anbar for Pure Science, 17(2): 210-224. https://doi.org/10.37652/juaps.2023.142363.1109
- [25] Aljarrah, R.M., Naamah, A.M., Alkhayatt, A.H.O. (2023). Concentration of spraying solution effect on the structural, morphological and optical properties of NiO thin films. Al-Bahir Journal for Engineering and Pure Sciences, 3(2): 4. https://doi.org/10.55810/2313-0083.1039